BBA - Bioenergetics 1860 (2019) 361–368

Contents lists available at ScienceDirect

BBA - Bioenergetics

journal homepage: www.elsevier.com/locate/bbabio

The carboxyl-terminal helical domain of the ATP synthase γ subunit is involved in ε subunit conformation and energy coupling☆

Atsuyoshi Yamakita[a], YingTao Liu[a], Masamitsu Futai[b], Atsuko Iwamoto-Kihara[a,*]

[a] Department of Bioscience, Nagahama Institute of Bio-Science and Technology, Nagahama, Shiga 526-0829, Japan
[b] Department of Biochemistry, Faculty of Pharmaceutical Sciences, Iwate Medical University, Yahaba, Iwate 028-3694, Japan

ARTICLE INFO

Keywords:
ATP synthase
F_1F_O-ATPase
Energy coupling
Mutagenesis
Cys-Cys cross-linking
Molecular motor

ABSTRACT

The γ subunit located at the center of ATP synthase (F_OF_1) plays critical roles in catalysis. *Escherichia coli* mutant with Pro substitution of the γ subunit residue γLeu218, which are located the rotor shaft near the *c* subunit ring, decreased NADH-driven ATP synthesis activity and ATP hydrolysis-dependent H^+ transport of membranes to ~60% and ~40% of the wild type, respectively, without affecting F_OF_1 assembly. Consistently, the mutant was defective in growth by oxidative phosphorylation, indicating that energy coupling is impaired by the mutation. The ε subunit conformations in the γLeu218Pro mutant enzyme were investigated by cross-linking between cysteine residues introduced into both the ε subunit (εCys118 and εCys134, in the second helix and the hook segment, respectively) and the γ subunit (γCys99 and γCys260, located in the globular domain and the carboxyl-terminal helix, respectively). In the presence of ADP, the two γ260 and ε134 cysteine residues formed a disulfide bond in both the γLeu218Pro mutant and the wild type, indicating that the hook segment of ε subunit penetrates into the $\alpha_3\beta_3$-ring along with the γ subunits in both enzymes. However, γ260/ε134 cross-linking in the γLeu218Pro mutant decreased significantly in the presence of ATP, whereas this effect was small in the wild type. These results suggested that the γ subunit carboxyl-terminal helix containing γLeu218 is involved in the conformation of the ε subunit hook region during ATP hydrolysis and, therefore, is required for energy coupling in F_OF_1.

1. Introduction

ATP synthase (F_OF_1), which is ubiquitous in the membranes of bacteria, mitochondria, and chloroplast thylakoids, synthesizes ATP coupling with an electrochemical proton gradient generated by the electron transport chain [1]. Bacterial enzymes are the simplest versions, consisting of a peripheral sector F_1 ($\alpha_3\beta_3\gamma\delta\varepsilon$) with three catalytic sites in the β subunits and an integral membrane F_O (ab_2c_{10-15}) with the H^+ pathway being formed by the *a* subunit and multiple *c* subunits (*c*-ring). Single-molecule observation of the *Escherichia coli* enzyme clearly indicates that the $\gamma\varepsilon c_{10}$ complex rotates against residual $\alpha_3\beta_3\delta ab_2$ during ATP hydrolysis [2–4]. Thus, ATP synthesis/hydrolysis is coupled to the reversible rotation that accompanies H^+ transport. The $\gamma\varepsilon c_{10}$ rotor should be elastic to connect different rotational steps in F_1 (120°, between three catalytic sites) and F_O (36°, between 10 proton binding sites) [5–7]. The crystal structure of *E. coli* F_1 revealed that the highly-extended carboxyl-terminal domain of ε subunit is inserted between the β and γ subunits *via* its Loop2/Helix2/Hook segments (Fig. 1A *left*) [8]. The extended conformation of the ε subunit corresponds with inhibition of rotation and ATP hydrolysis. On the other hand, the compact form ε has no inhibitory effect because its carboxyl-terminal domain does not interact with the catalytic β subunits (Fig. 1A *right*). The two ε conformations are thought to change reversibly depending on cellular conditions [9]. In addition, the ε subunit carboxyl-terminal domain probably contributes to lowering the activation energy of ATP hydrolysis for γ subunit rotation and bulk ATPase activity [10,11]. Therefore, consistent with the structure extending toward the β subunit, the ε subunit is pertinent for catalysis to proceed elementary steps smoothly through interactions with β and γ subunits [1]. However, it is unclear how the ε subunit changes its conformation and interacts with other subunits.

The γε subunit complex should interact with the catalytic β subunits for sequential steady-state catalysis and energy coupling. The amino- and carboxyl-terminal helices of the γ subunit form a coiled-coil

☆ This study was supported by JSPS KAKENHI Grant Number JP18570139. A research grant from Nagahama Institute of Bio-Science and Technology (to A. I–K) was also acknowledged.

* Corresponding author.
E-mail address: a_iwamoto@nagahama-i-bio.ac.jp (A. Iwamoto-Kihara).

https://doi.org/10.1016/j.bbabio.2019.03.002
Received 1 December 2018; Received in revised form 22 February 2019; Accepted 11 March 2019
Available online 12 March 2019
0005-2728/

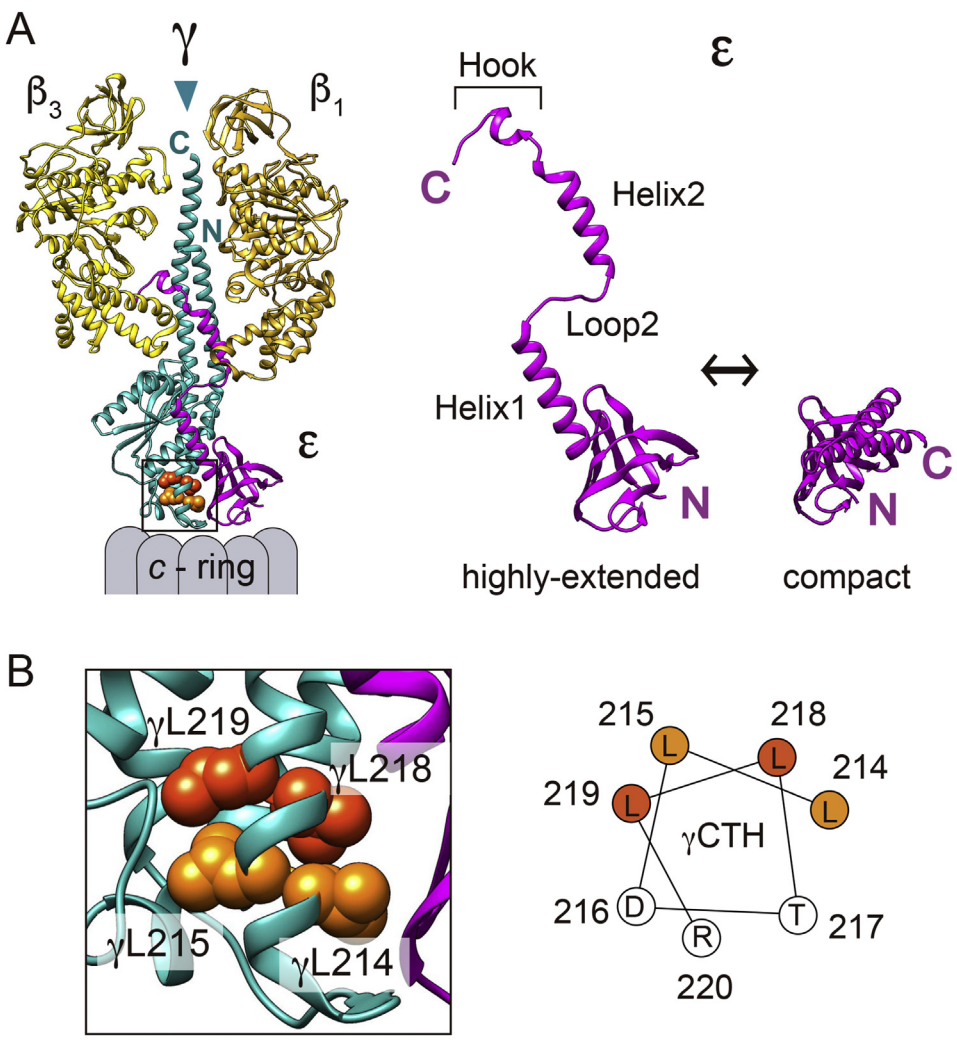

Fig. 1. Structure of the *E. coli* F_1 and the mutagenized γ subunit Leu residues. *A*, *Left,* Crystal structure of F_1 (PDB ID: 3OAA), β_1 and β_3 (yellow), γ (cyan), and ε (magenta) subunits are shown [8]. The γ and ε subunits are attached to the *c*-ring in the membrane, as schematically depicted. The γ subunit consists of amino- and carboxyl-terminal helices (both termini are indicated as "N" and "C" in the figure, respectively) and a globular domain. *Right,* The ε subunit consists of a β-sandwich domain and a α-helix domain of amino- and carboxyl-terminal parts, respectively [8]. The latter domain contains Helix1/Loop2/Helix2/Hook segments that are believed to change conformations between the extended and the compact forms. The structure of an isolated ε subunit (PDB ID: 1AQT) [34] is shown as the compact form. *B,* The area indicated by the square on Fig. 1A is enlarged. Leu residues, at positions 214, 215, 218, and 219, located in the γ carboxyl-terminal helix (γCTH) and Arg220 were substituted with Pro. The Leu residues are indicated in orange and red. The side-chains of these residues, except for Arg220, are facing the γ amino-terminal helix.

structure (Fig. 1, cyan). The γMet23Lys (γ subunit Met23 replaced with Lys) mutation in the amino-terminal helix increases the activation energy of rotation step and reduces the efficiency of energy coupling between H^+ transport and ATP hydrolysis by forming a salt bridge with the βGlu381 residue of the β subunit [12,13]. Mutations in the carboxyl-terminal helix reduce catalytic activity, however they can suppress the γMet23Lys mutation [14,15]. Therefore, the γ subunit's amino- and carboxyl-terminal helices are related to each other and should participate in the successive conformational changes of catalytic sites on each of the three β subunits, leading to energy coupling. As expected from the F_1 structure [8,16–18] and the inhibition of rotation by the ε carboxyl-terminal domain, the γ subunit should also interact with the ε subunit during energy coupling.

In this study, we isolated a series of γ subunit mutants defective in ATP synthesis. One of them, γLeu219Pro, located near the start of the carboxyl-terminal helix of the γ subunit, reduced energy coupling. This finding prompted us to introduce mutations into the helix, such as γLeu214Pro, γLeu215Pro, γLeu218Pro, and γArg220Pro, and to observe altered ATP-dependent ε-γ subunit interactions.

2. Materials and methods

2.1. Isolation of γ subunit mutants

Plasmid pBWU13.X, which carries all eight subunit genes of *E. coli* F_OF_1, and a null strain for F_OF_1 (DK8; *atpB-C ilv thi*) were used in this study [7]. Mutations were introduced randomly in the γ subunit gene using *Taq* DNA polymerase as reported previously [19]. The oxidative phosphorylation abilities of the mutant strains were tested at 37 °C on a minimal medium containing succinate (0.4%) or acetate (0.4%) as the sole carbon source [19,20]. To exclude assembly mutants unable to form ATP synthase (F_OF_1), western blotting of whole cell lysates or membranes was carried out using anti-F_1 antiserum. Mutants with single amino acid substitutions in the γ subunit genes were selected after DNA sequencing.

2.2. Site-directed mutagenesis of the γ and ε subunit genes

The site-directed Pro and Cys substitutions, γLeu214Pro, γLeu215Pro, γLeu218Pro, γArg220Pro, γLeu99Cys, and γLeu260Cys, were produced by replacing the *Kpn*I–*Spe*I segment of the γ subunit gene in pBWU13.X, with the DNA fragments that introduced codon changes by PCR using mutagenic primers (Table S1). Similarly, *Aor*51HI–*Xba*I fragments carrying εSer118Cys and εThr134Cys mutations of the ε subunit gene were used (Table S1). DNA sequences of resultant plasmids were verified to exclude mutations other than those introduced.

2.3. E. coli cultivation and preparation of inverted membrane vesicles

The plasmids carrying the wild-type and mutant F_OF_1 genes were introduced into *E. coli* DK8 cells. The cells were cultured at 37 °C, and their membranes were prepared using a French press [19,20]. Additionally, we cultured the cells at 25 °C to reduce the amount of F_OF_1 in

membranes (see Fig. S2). Ethylenediaminetetraacetic acid (EDTA) extracts rich in F_1 were prepared from membranes as described previously [19,20].

2.4. Measurements of ATP synthesis and hydrolysis

ATPase activities were assayed at 37 °C. Wild-type and mutant membranes (1–3 μg of membrane protein) were suspended in 0.3 ml of 20 mM Tris-HCl (pH 8.0) containing 140 mM KCl and 2 μg/ml bovine serum albumin. After incubation at 37 °C for 3 min, 0.3 ml of 20 mM Tris-HCl (pH 8.0) containing 8 mM ATP, 4 mM $MgCl_2$, and 140 mM KCl was added, incubated for 3–10 min, and then 0.3 ml of 1 N trichloroacetic acid was added to terminate reaction. The amount of inorganic phosphate was measured. Specific activities (μmoles ATP hydrolyzed per 1 mg total membrane proteins) are shown. Effects of LDAO and DCCD were also investigated [19,21]. After 15 min incubation at 25 °C with DCCD in 50 mM Tris-HCl, pH 7.5, containing 10 mM $MgCl_2$, an aliquot was subjected to an ATPase assay at 25 °C. ATP synthesis driven by NADH respiration was measured at 25 °C with 30 μg (protein) of inverted membranes in 0.4 ml of a solution of 50 mM MOPS-NaOH (pH 7.0), 5 mM $MgCl_2$, 6 mM inorganic phosphate, 2.1 mM NADH, and 0.6 mM ADP [22]. ADP was added 1 min after NADH addition. The reaction was terminated with the addition of trichloroacetic acid to 0.4 N and then was neutralized with 0.46 M Tris base solution. Aliquots of 50 μl were mixed with equal volume of solution from an ATP bioluminescence assay kit CLSII (Roche) [23,24]. NADH oxidation of the membranes was estimated at 25 °C by measuring absorbance at 340 nm with 100 μg (protein) of membranes in 2 ml of 50 mM MOPS-NaOH (pH 7.0), 5 mM $MgCl_2$, and 0.1 mM NADH [22].

2.5. Cross-linking between Cys residues introduced into the γ and ε subunits of wild-type and mutant membranes

Membranes (200 μg protein) suspended in 1.1 ml of 50 mM HEPES-NaOH (pH 7.5), 5 mM $MgCl_2$, and 10% glycerol were incubated with 10–100 μM $CuSO_4$ or 0.5–5 mM DTT (dithiothreitol) at 15 °C or 25 °C. Immediately after 5 min incubation, 0.1–1 mM EDTA was added to terminate the cross-linking reaction. Membranes were recovered by centrifugation (125,000 × *g* for 15 min) and suspended in the same buffer. The suspensions (20 μg protein) were subjected to 15% acrylamide gel electrophoresis in the presence of 0.1% sodium dodecyl sulfate without reducing agents. The proteins were transferred onto a PVDF membrane, and cross-linking between the γ and ε subunits was visualized using the antiserum against the γ or ε subunit. For testing nucleotide effects on cross-linking, membranes were incubated with 1–2 mM ADP, 1 mM ATP with 1 mM phosphoenolpyruvate and 50 μg/ml pyruvate kinase, or 1–2 mM AMP-PNP for 2 min prior to the addition of $CuSO_4$ or DTT.

2.6. Structure modeling of the γLeu218Pro mutant F_1

Tertiary structure of the γLeu218Pro mutant F_1 was estimated by homology modeling using the MOE software system (Ryoka Systems Inc., Tokyo, Japan) [25], based on the structure of *E. coli* F_1 (pdb: 3OAA) [8]. Fixing the regions of γLys9–γLys30, γGly75–γAsp83, γLeu86–γPhe95, γAsn174–γPro184, and γGln228–γGln263 of the γ subunit, energy minimization under an AMBER99 force field was carried out. The conformations of above regions were well conserved among F_1 crystal structures from bovines, yeast, and bacteria [8].

2.7. Other procedures

Protein concentrations were determined by the method outlined in Lowry et al. [26], using bovine serum albumin as a standard. H^+ transport was monitored by fluorescence quenching of acridine orange [19,20].

3. Results

3.1. The γLeu219Pro mutation is defective in energy coupling

We mutagenized the γ subunit gene to obtain strains defective in energy coupling between ATP synthesis (or hydrolysis) and the electrochemical proton gradient. The strain harboring a single γLeu219Pro mutation (γ subunit Leu219 replaced by Pro) was identified from 91 mutants that hardly or never grew by oxidative phosphorylation at 37 °C. The membranes prepared exhibited ~80% of the wild-type ATPase activity, whereas its H^+ translocation was ~20% of wild type. Thus, we became interested in the γLeu219 residue and its immediate vicinity in the long carboxyl-terminal helix where the residue was located (Fig. 1A *left* and B).

3.2. Proline substitutions of residues near γLeu219

We substituted Leu residues (γLeu214, γLeu215, and γLeu218) in the vicinity of γLeu219 that faced the amino-terminal helix of γ subunit (Fig. 1B). γArg220 at the opposite side of the helix was also replaced (Fig. 1B *right*). Similar to γLeu219Pro, γLeu214Pro and γLeu218Pro mutants grew slowly under oxidative phosphorylation with ≤20% of the wild-type growth yield (Fig. S1), whereas γArg220Pro exhibited wild-type growth. The mutant membranes contained essentially the same amount of F_1 as those from the wild type grown at 37 °C, except that the F_1 content of γLeu219Pro was slightly reduced (~70% of wild type) (Fig. S2A). Thus, the γ subunit carrying Leu214Pro or Leu218Pro could not support growth even though assembly of the mutant F_OF_1 was essentially the same as the wild type. These results suggested that the Pro residue at position γ214 or γ218 impaired energy coupled ATP synthesis *in vivo*.

We tested membranes of the mutant strains cultured at 25 °C, which contained essentially the same amount of F_1 as the wild type cultured at the same temperature (Fig. S2B). ATPase activities of the wild type membranes were 2.4 and 5.3 μmol/mg·min when the cells were grown at 25 °C and 37 °C, respectively (Table I). Immunoblotting also showed the amount of F_1 subunit increased with temperature (Fig. S2C), consistent with the elevated ATPase activity at 37 °C. These results were probably due to an increased copy number of the plasmid harboring the F_OF_1 genes at 37 °C since plasmid replication is temperature dependent given the lack of the *rop* gene [27,28].

Interestingly, the membranes from γLeu214Pro, γLeu215Pro, and γLeu218Pro mutants grown at 37 °C exhibited about 2-fold higher ATP hydrolysis than those of the wild type, although their ATP-driven H^+ transport was 60%–80% (Table I). Typically, γLeu218Pro membranes containing essentially the same amount of F_1 as the wild type had 2-fold higher ATPase activity, while H^+ transport was ~60%. Similar results were obtained with the membranes from cells cultured at 25 °C: the Leu218Pro membranes failed to pump enough H^+ corresponding to the ATPase activity (Table I; 1.3-fold ATPase compared to the wild type but ~50% H^+ transport). Thus, ATP hydrolysis of these mutant enzymes was partially uncoupled to H^+ transport. These findings prompted us to study γLeu218Pro F_OF_1 in membranes.

The membrane ATPases of γLeu218Pro mutant and the wild type were inhibited with *N,N′*-dicyclohexylcarbodiimide (DCCD), which binds to the Asp61 residue of the F_O *c* subunit [29]. Despite the presence of the same amount of F_1 in the wild-type and γLeu218Pro membranes, residual ATPase activities of 20 μM DCCD treatments were 19 ± 5% ($n = 4$) and 35 ± 7% ($n = 3$), respectively. Thus, γLeu218Pro mutation may evoke defective coupling between the H^+-pathway and catalytic sites in F_OF_1.

As expected, the ATP synthesis rate of the γLeu218Pro membranes was about 36% of that of the wild type when an electrochemical H^+ gradient was generated with NADH (Table I). ATP synthesis by other mutants, except for γArg220Pro, was also reduced (71%–78% of wild type), whereas NADH oxidation rates of all mutants were essentially the

Table I
Activities of membranes from γ subunit mutants with Pro substitutions.

Strain	Hydrolysis		H^+ transport		Synthesis	H^+/Hyd	Syn/Hyd
	37°C	25°C	37°C	25°C	25°C	25°C	25°C
	μmol/mg·min		%		nmol/mg·min	Relative value	
	(*n* = 8)	(n = 3)	(n = 4)	(n = 3)	(n = 3)		
Wild type	5.3 ± 0.4	2.4 ± 0.1	100	100	4.5 ± 0.7	1	1
γLeu214Pro	9.5 ± 0.4	3.4 ± 0.2	84 ± 6	76 ± 3	3.4 ± 0.2	0.53	0.52
γLeu215Pro	9.4 ± 0.5	2.9 ± 0.4	82 ± 7	80 ± 6	3.5 ± 0.4	0.66	0.64
γLeu218Pro	11 ± 0.5	3.1 ± 0.2	57 ± 8	52 ± 3	1.6 ± 0.1	0.39	0.27
γLeu219Pro	4.6 ± 0.4	2.2 ± 0.3	25 ± 6	69 ± 6	3.2 ± 0.5	0.75	0.79
γArg220Pro	5.0 ± 0.6	1.9 ± 0.4	96 ± 4	84 ± 10	4.6 ± 1.0	1.1	1.3

Inverted membranes from the wild-type and the mutant strains of ATP synthase γ subunit were prepared using *E. coli* cells cultured at 37 °C or 25 °C in minimal media containing 0.5% glycerol or 0.4% glucose as the sole carbon source, respectively. ATP hydrolysis, ATP-dependent H^+ transport, and NADH-dependent ATP synthesis of the membranes were exhibited with standard error. H^+-transport is shown as the relative amount of final extent of the fluorescence quenching at the same time after addition of ATP. H^+ transport/ATP hydrolysis (H^+/Hyd) and ATP synthesis/ATP hydrolysis (Syn/Hyd) efficiencies were calculated by comparing each ratio of mutant/wild-type activity. At lower culture temperature, the amounts of F_OF_1 decreased (Fig. S2) because of reduced plasmid copy number [27,28].

same as that of the wild type (1.4–1.8 μmol/mg·min). Thus, the γLeu218Pro mutation significantly reduced energy coupling between the electrochemical H^+ gradient and ATP synthesis, leading to slow growth dependent on oxidative phosphorylation (Fig. S1). These results suggested that γLeu218 is involved in energy coupling with the residues in its vicinity.

3.3. Effects of LDAO on ATPase activities of Leu-to-Pro mutants

The detergent lauryldimethylamine *N*-oxide (LDAO) stimulates ATPase activity by relieving the inhibitory effects of the ε subunit and ADP [21,30]. The membrane ATPase activities of wild type and γArg220Pro mutant increased > 2.5-fold with 3 mM LDAO (Fig. 2A). However, activities of mutants with Leu-to-Pro replacements (Leu-to-Pro mutants) increased < 2-fold (Fig. 2A).

LDAO increased the F_1-ATPase activities of wild type and the γArg220Pro mutant about 3.5-fold but had essentially no effect on the Leu-to-Pro mutants (Fig. 2B). These results suggested that the inhibition by the ε subunit was reduced in the Pro mutations. Thus, the Pro mutations, including γLeu218Pro, possibly affected the conformation of the ε carboxyl-terminal domain, which is involved in ATPase inhibition, perhaps by reducing its interaction with the β or γ subunits. Therefore, it became of interest to study the conformation and interactions of the ε subunit in the Pro mutant enzymes.

3.4. Detection of ε subunit extended conformation in the wild-type and the γLeu218Pro enzymes

We selected the γLeu218Pro mutation, which exhibited the most defective energy coupling among the four Leu-to-Pro mutants studied. As Table I shows, the calculated H^+-transport/hydrolysis and ATP synthesis/hydrolysis ratios (H^+/Hyd and Syn/Hyd, respectively) of the mutant were ~30% of the wild type. We studied the conformations of the ε subunit, focusing on two pairs of γ and ε residues located closely or distantly (γ260/ε134 and γ99/ε118; 6.2 Å and 28.3 Å Cα-Cα distances, respectively), by replacing them with Cys residues (Fig. 3). In F_1 with a highly-extended ε subunit, the γ260/ε134 pair is in close proximity, whereas the γ99/ε118 pair is distant. Growth by oxidative phosphorylation was scarcely affected by the Cys substitutions in the strain having the wild-type γ subunit (γLeu218) or the mutant γ subunit (γPro218). Thus, they could be used to probe the interaction of γ/ε subunits.

Cross-linking of the γ/ε pairs were conducted by oxidizing the Cys residues in membrane-bound F_OF_1 with $CuSO_4$ at 15 °C. Cross-linking of γCys260/εCys134 was detected in the wild-type (γLeu218) membranes by western blotting using antibodies against the γ or ε subunit and identifying the γ-ε dimer of about 45 kDa (Fig. 4A). This result suggested that the distance between γ260 and ε134 in membrane-bound F_OF_1 is very close as shown in the crystal structure [8]. Although

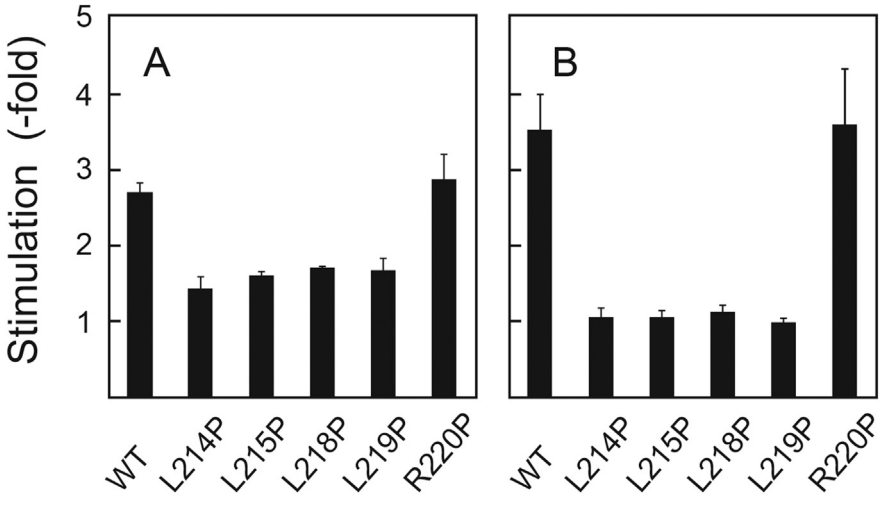

Fig. 2. Effects of LDAO on the ATPase activities of membranes and partially purified F_1. ATPase activities of the membranes (*A*) and the partially purified F_1 (*B*) from the wild type and the mutants were assayed at 37 °C in the presence or absence of 3 mM LDAO. ATPase stimulation by LDAO was shown with standard error (*n* = 3).

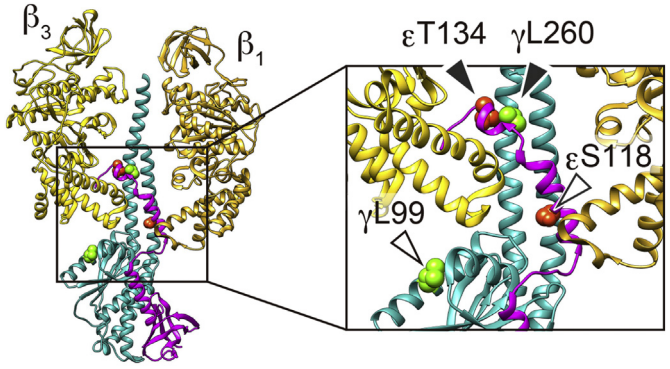

Fig. 3. Conformation of the ε subunit and the sites of Cys replacement in the ε and γ subunits. The region indicated by a square on F_1 (left) is enlarged (right). The residues indicated by spheres in light-green (γLeu99 and γLeu260) and red (εSer118 and εThr134) were substituted with Cys in combinations of γ99/ε118 (open triangles) and γ260/ε134 (closed triangles) for γ-ε subunit cross-linking. The distances between the Cα of the amino acid pairs of γLeu260-εThe134 and γLeu99-εSer118 are about 6.2 Å and 28.3 Å, respectively.

γCys99 and εCys118 were cross-linked, a significant amount of the γ and ε subunits remained unconjugated, suggesting that γ99/ε118 is more distant than γ260/ε134 but occasionally come close enough together to be cross-linked (Fig. 4A). At a higher temperature (25 °C), the γ99/ε118 cross-linking increased significantly (Fig. 4B, WT), suggesting that the carboxyl-terminal εHelix2/εHook (εVal112–εIle125/εAla126–εMet138) of the ε subunit containing ε118 and ε134 is not strictly fixed and is susceptible to thermal fluctuations. Cross-linked γ260/ε134 and γ99/ε118 were also detected in γPro218 mutant membranes with no significant difference from the wild type (Fig. 4B, Mutant). Thus, the γLeu218Pro mutation does not prevent the ε subunit from forming the highly-extended conformation.

3.5. Effects of nucleotides on the extended conformation of the ε subunit

It became of interest to know whether γ260/ε134 cross-linking is affected by ADP and ATP because the γLeu218Pro mutant exhibited elevated ATPase activity (Table I). About 97% and 92% of γCys260 of the wild-type and mutant F_OF_1 were cross-linked with εCys134, respectively, when membranes were treated in the presence of ADP (Fig. 5A, purple and green bars are indicating wild type (γLeu218) and mutant (γPro218), respectively).

Cross-linking of the wild type decreased to ~80% with adenosine 5′-(β,γ-imido)triphosphate (AMP-PNP; a non-hydrolyzable ATP analog) or ATP (with regeneration system, ref. 7) (Fig. 5A, purple bar). It should be noted that the $CuSO_4$ concentration (10 μM) was nearly saturating for γ260/ε134 cross-linking in the presence of ATP (Fig. S3). Fig. 5A also shows that the γPro218 mutation decreased cross-linking to a greater extent (decreased to 72% and 63% with AMP-PNP and ATP, respectively; in Fig. 5A, green bar) suggesting that the conformation of the ε subunit is affected by the γPro218 mutation depending on the presence of ATP. However, we do not currently know the location of the ε carboxyl-terminal domain when it is not highly extended.

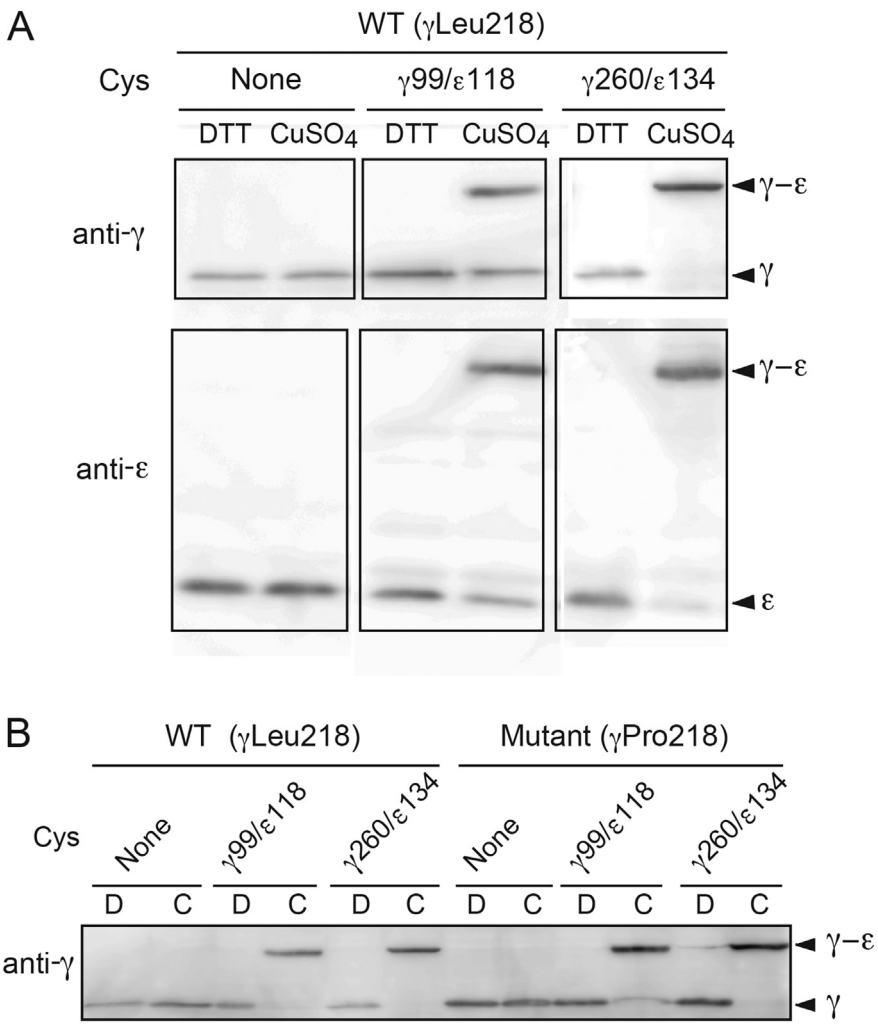

Fig. 4. Cross-linking between Cys residues introduced into the γ and ε subunits of the wild type (γLeu218) and the mutant (γPro218). Cross-link formation between the two sets of Cys residues introduced at γLeu99/εSer118 and γLeu260/εThr134 is shown. *A*, Inverted membranes (200 μg protein) of the wild type having γLeu218 were incubated with 100 μM $CuSO_4$ or 5 mM DTT at 15 °C. The reaction with stopped with 1 mM EDTA, and aliquots (20 μg) were subjected to 15% acrylamide gel electrophoresis containing 0.1% SDS. Immunoblotting using antisera against γ and ε subunits was carried out. *B*, Two Cys pairs of the wild-type (γLeu218) and the mutant (γPro218) membranes were cross-linked at 25 °C for 5 min, as described for *A*. Cross-link formation was detected with anti-γ subunit antiserum. D, with DTT; C, with $CuSO_4$.

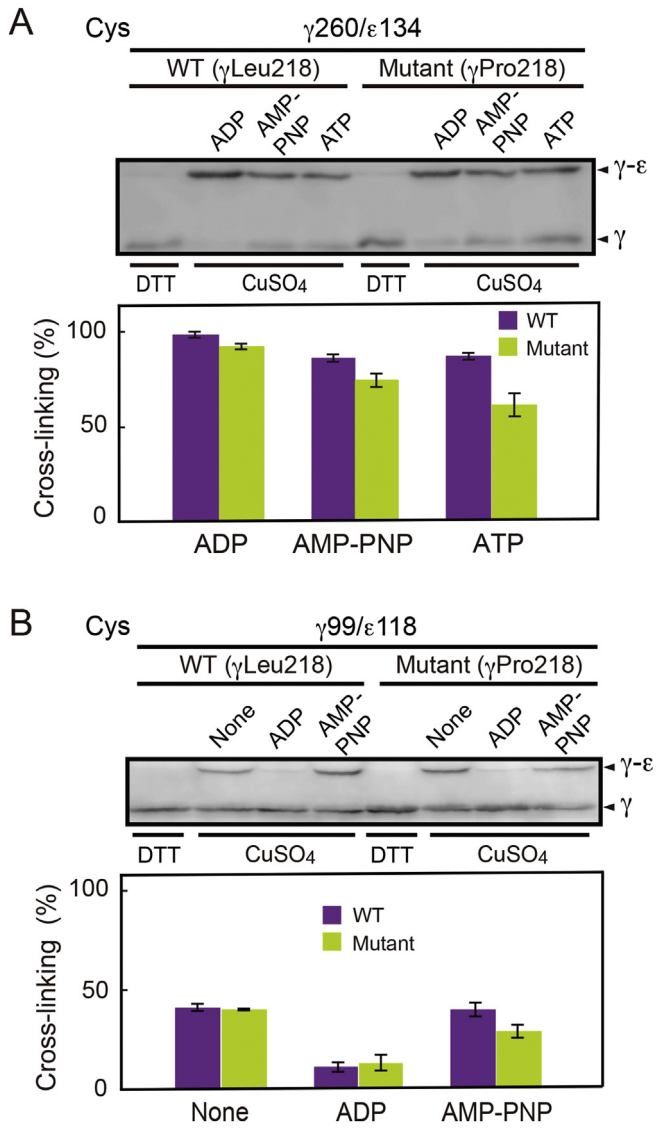

Fig. 5. Effects of nucleotides on γ/ε subunit cross-linking of the wild-type (γLeu218) and mutant (γPro218) membranes. *A*, Inverted membranes (200 μg protein) of the wild type (WT, purple) and the mutant (yellowish-green) containing Cys residues at γ260/ε134 were incubated with or without 1 mM nucleotides for 2 min at 25 °C, before addition of 10 μM $CuSO_4$ or 0.5 mM DTT. After 5 min incubation at the same temperature, EDTA was added to 0.1 mM. Aliquots (15 μg protein) were subjected to 12% acrylamide gel electrophoresis and immunoblotting. The ratio of cross-linking was estimated by densities of the γ-ε subunit bands. An average of three experiments is shown with standard error. *B*, Wild-type (WT) and mutant membranes with Cys residues at γ99/ε118 were tested for cross-linking. Experimental conditions were modified: 2 mM nucleotides, 100 μM $CuSO_4$ or 5 mM DTT, and 1 mM EDTA. Incubation temperature was 15 °C instead of 25 °C. Aliquots (15 μg protein) were subjected to 15% acrylamide gel electrophoresis and immunoblotting.

We also examined whether γ99/ε118 cross-linking (Fig. 4A) is affected by nucleotides. About 40% of the γ subunits of the wild-type and mutant F_OF_1 were cross-linked in the absence of nucleotides at 15 °C (Fig. 5B); however, this rose to 91% at 25 °C, as estimated from Fig. 4B, suggesting that the distance between γCys99 and εCys118 changes with thermal fluctuations of the ε subunit carboxyl-terminal structure. Cross-linking decreased to about 10% with the addition of ADP (Fig. 5B), suggesting that the two Cys residues became more distant in the presence of ADP. However, AMP-PNP did not substantially affect cross-linking, 40 ± 11% and 29 ± 10% in the wild-type and mutant enzymes, respectively (Fig. 5B).

4. Discussion

A series of studies have indicated that the γ subunit regulates energy coupling between ATP hydrolysis/synthesis and H^+ transport through the rotation of the ε/γ and *c* subunit ring [12–15]. However, the detailed mechanism of this process is still unknown. In this study, we have investigated roles of the γ subunit helical domain by introducing Pro mutations such as γLeu218Pro (Fig. 1). As expected, the γ subunit carboxyl-terminal helix, which includes γLeu218, is involved in energy coupling through the ε carboxyl-terminal domain.

Pro residues function as "helix breakers," since they are usually found at the termini or in the kinks of α-helices [31,32]. Consistent with probable structural alterations, the Leu-to-Pro mutant γ subunits migrated slightly slower than the wild-type γ during acrylamide gel electrophoresis (Fig. S2A, arrow). Simulation of γ subunit structure with the γPro218 mutation based on the *E. coli* F_1 crystal structure [8] predicts a random loop between γLeu214 and γThr217 instead of the wild-type helix (not shown). Since other Pro mutations also affected ATP-dependent H^+ pumping and ATP synthesis (Fig. 1, Table I), the carboxyl-terminal helix of the γ subunit, especially the region closest to the ε subunit amino-terminal domain and *c*-ring, should play significant roles in coupled rotational catalysis.

According to the crystal structure of *E. coli* F_1, the γ subunit is assembled with the highly-extended ε subunit in the center of $\alpha_3\beta_3$-ring [8]. Only one nucleotide (ADP) binds to β_1, which is regarded as the equivalent of the ADP-binding β_{DP} subunit of mitochondrial F_1 [16]. Although two other β subunits do not bind nucleotides, β_2 and β_3, are similar to the mitochondrial β_E (empty of a nucleotide) and β_{TP} (ATP-binding) subunits [16], respectively, judging from their conformations and interactions with an asymmetric γ subunit [8]. The ε subunit is inserted between the β and γ subunits with its carboxyl-terminal segments (εLoop2/εHelix2/εHook) (Fig. 1A *left*) [8].

As a schematic model of Fig. 6A shows, based on the crystal structure, the εHook and the εHelix2/εLoop2 segments interact with β_3 and β_1 subunits, respectively (Fig. 6A, upper and lower dotted circles). The cysteines at γ260 (in γ carboxyl-terminal helix) and ε134 (in εHook) were readily cross-linked in the membrane F_OF_1 without addition of ATP or ADP (Fig. 4B), consistent with the spatial arrangement of γLeu260 and εAla134 in the crystal structure (Figs. 3 and 6A, closed arrow-heads). Fixing the ε subunit in the highly-extended form by γ260/ε134 cross-linking reduced ATPase activity (Fig. S3, solid line), which may be due to rotation inhibition caused by stabilized interactions between stator (β) and rotor (ε/γ). Consistent with this finding, the inhibitory interaction between βGlu381 (in β_1) and εSer108 (in εLoop2) was demonstrated previously [11] (Fig. 6A, lower dotted circle).

Although the γ99/ε118 is distant in the crystal structure (Fig. 3, open arrow-heads), the introduced cysteines were cross-linked in the wild-type enzyme, which increased in a temperature-dependent manner (Fig. 4). Thus, the εHelix2 (containing ε118) conformationally fluctuates together with the εHook (containing ε134) to allow cross-linking with the γ globular domain (γ99) (Fig. 6B, open arrow-heads).

In the presence of millimolar concentrations of ATP, at least two nucleotides bind to the catalytic sites of two β subunits, as previously demonstrated [33], though the β_3 subunit in the F_1 crystal structure have no bound ATP but rather interacts with the εHook (Fig. 6A, upper dotted circle). Thus, ATP binding to the β_3 should change its conformation and lower the interaction between β_3 and εHook. It became of interest to study the effects of nucleotides on the ε subunit conformation by using γ/ε subunit cross-linking of the membrane F_OF_1.

As expected, the γ260/ε134 cross-linking was reduced to ~80% in the presence of ATP (plus Mg^{2+} with a regenerating system) or AMP-PNP (Fig. 5A). This result suggested that the binding of ATP to a β subunit (probably β_3) decreased the interaction between β_3 and εHook, so that the ε134 became located distantly away from the γ260 by altering the ε conformation (Fig. 6C). As described above, the

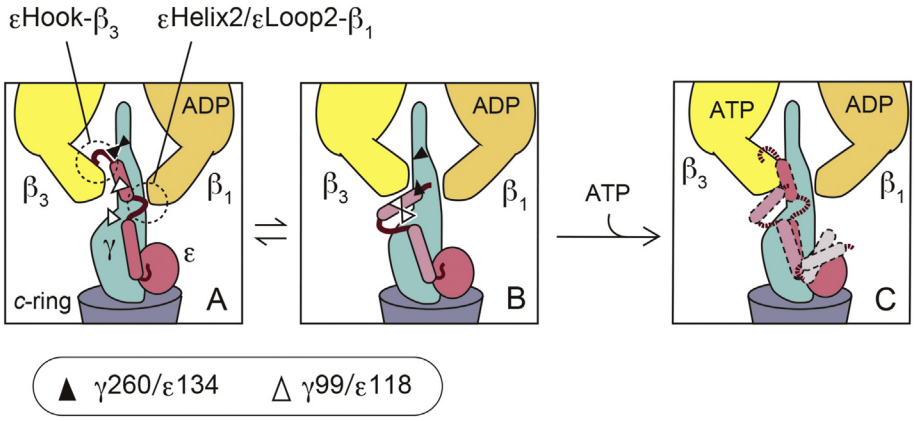

Fig. 6. Scheme of β-ε interactions in the F_OF_1. *A*, According to the crystal structure of *E. coli* F_1 [8], the carboxyl-terminal domain of ε subunit is highly-extended and interacts with the β_3 subunit bound no nucleotide and the β_1 subunit bound ADP through the εHook and the εLoop2/εHelix2 segments, respectively, as indicated by dotted circles. The positions of γ260 and ε134 (closed arrowheads) are enough close to be cross-linked. *B*. However, the conformation of εHook/εLoop2/εHelix2 segments flexibly changes to allow γ99/ε118 cross-linking (open arrowheads) in membrane F_OF_1. *C*. ATP binding to the β_3 subunit increases flexibility of the ε subunit segments, especially in γLeu218Pro mutant F_OF_1. Since both of the γ260/ε134 and γ99/ε118 cross-linkings are decreased in the mutant, the ε segments transiently change the conformation including a compact form (light-gray with dashed line) from those in panel A and B (pink and light-pink with dashed line, respectively). The β_1, β_3, γ, and ε subunits are shown in orange, yellow, light-blue and pink, respectively. The β_2 subunit bound no nucleotide is not shown here. The *c*-ring is also shown in grayish-blue. In panel C, arrowheads indicating γ260/ε134 and γ99/ε118 are omitted.

γLeu218Pro mutation decreased γ260/ε134 cross-linking to 63% and 72% upon addition of ATP and AMP-PNP, respectively, suggesting that ATP binding to the mutant enzyme significantly affects the interaction between β_3 and ε. Thus, the altered interaction between the β subunit and the γ/ε rotor in the γPro218 mutant led to defective energy coupling. In fact, the mutant ATPase activity was ~2-fold higher but had 60% of the wild-type H^+ transport ability (Table I). It is still unknown where the εHelix2/εHook region is located in F_1 when the ε subunit was not highly extended. One possibility is that the region interacts with εHelix1 to form the compact conformation (Fig. 1A *right*) [34]. However, the γ260/ε134 cross-linking still significant in the presence of ATP or AMP-PNP (Fig. 5A), suggesting that the compact conformation is not maintained for several minutes upon $CuCl_2$ treatment. Thus, ATP binding probably reduces stability of the extended form of the ε subunit and induces its transient forms including the compact one (Fig. 1C).

ADP did not decrease the cross-linking of γ260/ε134 in the wild type or mutant F_OF_1 (Fig. 5A) possibly because the conformation of β_3 in the enzyme does not change to release the εHook. Thus, the highly-extended ε subunit along with the γ subunit's helix is stable when ADP is bound to F_1, regardless of wild-type or mutants. It has been previously reported that the ε subunit does not readily dissociate from *E. coli* F_1 when Mg·ADP plus phosphate are bound [35]. ADP clearly decreased the cross-linking of γ99/ε118 in the wild type and mutant F_OF_1 (Fig. 5B). Since the conformational fluctuation of the ε subunit is reduced in the presence of ADP, ε118 and γ99 are located distantly apart, as shown in Fig. 3.

The γLeu218Pro mutant exhibited low ATP synthesis and ATP-dependent H^+ transport but almost 2-fold increased ATPase activity, suggesting that the mutation affects rotor properties. Similar results were obtained with the cross-linking of Cys residues introduced into γTyr207 and *c*Gln42 located near the start of the γ subunit's carboxyl-terminal helix (γPro211–γVal286) and the *c* subunit loops between two trans-membrane helices, respectively [36]. Mutations in the *c* subunit loop also affect energy coupling [37]. Thus, the region connecting between the γ subunit and *c*-ring is important in energy coupling. These results also suggested that the rotor ($\gamma\varepsilon c_{10}$) has flexibility and elasticity in ATP-dependent rotation [7].

Conflict of interest

The authors declare that they have no conflicts of interest with the contents of this article.

Transparency document

The Transparency document associated with this article can be found, in online version.

Acknowledgements

The authors are grateful to Yoshinori Kimura, Kouki Toda, and Naoto Dobashi for technical assistance with the experiments. We also thank to Dr. Ken-Ich Takahashi for advice with the structural simulations. We would like to thank Enago (www.enago.jp) for the English language review.

Appendix A. Supplementary data

Supplementary data to this article can be found online at https://doi.org/10.1016/j.bbabio.2019.03.002.

References

[1] M. Nakanishi-Matsui, M. Sekiya, M. Futai, ATP synthase from Escherichia coli: mechanism of rotational catalysis, and inhibition with the epsilon subunit and phytopolyphenols, Biochim. Biophys. Acta 1857 (2016) 129–140.
[2] Y. Sambongi, Y. Iko, M. Tanabe, H. Omote, A. Iwamoto-Kihara, I. Ueda, T. Yanagida, Y. Wada, M. Futai, Mechanical rotation of the *c* subunit oligomer in ATP synthase (F_0F_1): direct observation, Science 286 (1999) 1722–1724.
[3] M. Tanabe, K. Nishio, Y. Iko, Y. Sambongi, A. Iwamoto-Kihara, Y. Wada, M. Futai, Rotation of a complex of the gamma subunit and c ring of Escherichia coli ATP synthase. The rotor and stator are interchangeable, J. Biol. Chem. 276 (2001) 15269–15274.
[4] K. Nishio, A. Iwamoto-Kihara, A. Yamamoto, Y. Wada, M. Futai, Subunit rotation of ATP synthase embedded in membranes: a or beta subunit rotation relative to the *c* subunit ring, Proc. Natl. Acad. Sci. U. S. A. 99 (2002) 13448–13452.
[5] M.G. Duser, N. Zarrabi, D.J. Cipriano, S. Ernst, G.D. Glick, S.D. Dunn, M. Borsch, 36 degrees step size of proton-driven *c*-ring rotation in FoF_1-ATP synthase, EMBO J. 28 (2009) 2689–2696.
[6] M. Diez, B. Zimmermann, M. Borsch, M. Konig, E. Schweinberger, S. Steigmiller, R. Reuter, S. Felekyan, V. Kudryavtsev, C.A. Seidel, P. Graber, Proton-powered subunit rotation in single membrane-bound F_0F_1-ATP synthase, Nat. Struct. Mol. Biol. 11 (2004) 135–141.
[7] H. Oka, H. Hosokawa, M. Nakanishi-Matsui, S.D. Dunn, M. Futai, A. Iwamoto-Kihara, Elastic rotation of Escherichia coli F_OF_1 having epsilon subunit fused with cytochrome b_{562} or flavodoxin reductase, Biochem. Biophys. Res. Commun. 446 (2014) 889–893.
[8] G. Cingolani, T.M. Duncan, Structure of the ATP synthase catalytic complex F_1 from *Escherichia coli* in an autoinhibited conformation, Nat. Struct. Mol. Biol. 18 (2011) 701–707.
[9] S.P. Tsunoda, A.J. Rodgers, R. Aggeler, M.C. Wilce, M. Yoshida, R.A. Capaldi, Large conformational changes of the epsilon subunit in the bacterial F_1F_0 ATP synthase provide a ratchet action to regulate this rotary motor enzyme, Proc. Natl. Acad. Sci. U. S. A. 98 (2001) 6560–6564.
[10] M. Sekiya, H. Hosokawa, M. Nakanishi-Matsui, M.K. Al-Shawi, R.K. Nakamoto, M. Futai, Single molecule behavior of inhibited and active states of *Escherichia coli* ATP synthase F_1 rotation, J. Biol. Chem. 285 (2010) 42058–42067.
[11] M. Nakanishi-Matsui, M. Sekiya, S. Yano, M. Futai, Inhibition of F_1-ATPase rotational catalysis by the carboxyl-terminal domain of the subunit, J. Biol. Chem. 289 (2014) 30822–30831.
[12] M.K. Al-Shawi, C.J. Ketchum, R.K. Nakamoto, Energy coupling, turnover, and

stability of the F_0F_1 ATP synthase are dependent on the energy of interaction between gamma and beta subunits, J. Biol. Chem. 272 (1997) 2300–2306.
[13] M. Sekiya, R.K. Nakamoto, M.K. Al-Shawi, M. Nakanishi-Matsui, M. Futai, Temperature dependence of single molecule rotation of the *Escherichia coli* ATP synthase F_1 sector reveals the importance of gamma-beta subunit interactions in the catalytic dwell, J. Biol. Chem. 284 (2009) 22401–22410.
[14] A. Iwamoto, J. Miki, M. Maeda, M. Futai, H^+-ATPase gamma subunit of *Escherichia coli*, Role of the conserved carboxyl-terminal region, J. Biol. Chem. 265 (1990) 5043–5048.
[15] R.K. Nakamoto, M. Maeda, M. Futai, The gamma subunit of the *Escherichia coli* ATP synthase. Mutations in the carboxyl-terminal region restore energy coupling to the amino-terminal mutant gamma Met-23→Lys, J. Biol. Chem. 268 (1993) 867–872.
[16] J.P. Abrahams, A.G.W. Leslie, R. Lutter, J.E. Walker, Structure at 2.8 Å resolution of F_1-ATPase from bovine heart mitochondria, Nature 370 (1994) 621–628.
[17] R.I. Menz, J.E. Walker, A.G.W. Leslie, Structure of bovine mitochondrial F_1-ATPase with nucleotide bound to all three catalytic sites, Cell 106 (2001) 331–341.
[18] Y. Shirakihara, A. Shiratori, H. Tanikawa, M. Nakasako, M. Yoshida, T. Suzuki, Structure of a thermophilic F_1-ATPase inhibited by an epsilon-subunit: deeper insight into the epsilon-inhibition mechanism, FEBS J. 282 (2015) 2895–2913.
[19] A. Iwamoto, M.Y. Park, M. Maeda, M. Futai, Domains near ATP gamma phosphate in the catalytic site of H^+-ATPase, Model proposed from mutagenesis and inhibitor studies, J. Biol. Chem. 268 (1993) 3156–3160.
[20] A. Iwamoto, H. Omote, H. Hanada, N. Tomioka, A. Itai, M. Maeda, M. Futai, Mutations in Ser174 and the glycine-rich sequence (Gly149, Gly150, and Thr156) in the beta subunit of *Escherichia coli* H^+-ATPase, J. Biol. Chem. 266 (1991) 16350–16355.
[21] S.D. Dunn, R.G. Tozer, V.D. Zadorozny, Activation of *Escherichia coli* F_1-ATPase by lauryldimethylamine oxide and ethylene glycol: relationship of ATPase activity to the interaction of the epsilon and beta subunits, Biochemistry 29 (1990) 4335–4340.
[22] P.C. Jones, Introduction of a carboxyl group in the first transmembrane helix of *Escherichia coli* F_1F_O ATPase subunit *c* and cytoplasmic pH regulation, J. Bacteriol. 183 (2001) 1524–1530.
[23] J.J. Tomashek, O.B. Glagoleva, W.S. Brusilow, The *Escherichia coli* F_1F_0 ATP synthase displays biphasic synthesis kinetics, J. Biol. Chem. 279 (2004) 4465–4470.
[24] T. Suzuki, Y. Ozaki, N. Sone, B.A. Feniouk, M. Yoshida, The product of *unc*I gene in F_1F_O-ATP synthase operon plays a chaperone-like role to assist *c*-ring assembly, Proc. Natl. Acad. Sci. U. S. A. 104 (2007) 20776–20781.
[25] Y. Sasaki, E. Nogami, M. Maeda, M. Nakanishi-Matsui, A. Iwamoto-Kihara, A unique F-type H^+-ATPase from *Streptococcus mutans*: an active H^+ pump at acidic pH, Biochem. Biophys. Res. Commun. 443 (2014) 677–682.
[26] O.H. Lowry, N.J. Rosebrough, A.L. Farr, R.J. Randall, Protein measurement with the Folin phenol reagent, J. Biol. Chem. 193 (1951) 265–275.
[27] Y. Moriyama, A. Iwamoto, H. Hanada, M. Maeda, M. Futai, One-step purification of *Escherichia coli* H^+-ATPase (F_0F_1) and its reconstitution into liposomes with neurotransmitter transporters, J. Biol. Chem. 266 (1991) 22141–22146.
[28] S. Lin-Chao, W.T. Chen, T.T. Wong, High copy number of the pUC plasmid results from a Rom/Rop-suppressible point mutation in RNA II, Mol. Microbiol. 6 (1992) 3385–3393.
[29] W. Sebald, W. Machleidt, E. Wachter, *N,N′*-dicyclohexylcarbodiimide binds specifically to a single glutamyl residue of the proteolipid subunit of the mitochondrial adenosinetriphosphatases from *Neurospora crassa* and *Saccharomyces cerevisiae*, Proc. Natl. Acad. Sci. U. S. A. 77 (1980) 785–789.
[30] H.R. Lotscher, C. deJong, R.A. Capaldi, Interconversion of high and low adenosinetriphosphatase activity forms of *Escherichia coli* F_1 by the detergent lauryldimethylamine oxide, Biochemistry 23 (1984) 4140–4143.
[31] A. Senes, D.E. Engel, W.F. DeGrado, Folding of helical membrane proteins: the role of polar, GxxxG-like and proline motifs, Curr. Opin. Struct. Biol. 14 (2004) 465–479.
[32] J. Abramson, H.R. Kaback, S. Iwata, Structural comparison of lactose permease and the glycerol-3-phosphate antiporter: members of the major facilitator superfamily, Curr. Opin. Struct. Biol. 14 (2004) 413–419.
[33] H. Hanada, T. Noumi, M. Maeda, M. Futai, Uni-site catalysis by *Escherichia coli* F_1-ATPase with different numbers of bound nucleotides, FEBS Lett. 257 (1989) 465–467.
[34] Uhlin, U., Cox, G. B., and Guss, J. M. (1997) Crystal structure of the epsilon subunit of the proton-translocating ATP synthase from *Escherichia coli*. Structure (London, England: 1993) 5, 1219-1230.
[35] N.B. Shah, M.L. Hutcheon, B.K. Haarer, T.M. Duncan, F_1-ATPase of *Escherichia coli*: the epsilon-inhibited state forms after ATP hydrolysis, is distinct from the ADP-inhibited state, and responds dynamically to catalytic site ligands, J. Biol. Chem. 288 (2013) 9383–9395.
[36] B. Schulenberg, R. Aggeler, J. Murray, R.A. Capaldi, The γε*c* subunit interface in the ATP synthase of *Escherichia coli*. cross-linking of the epsilon subunit to the c subunit ring does not impair enzyme function, that of gamma to *c* subunits leads to uncoupling, J. Biol. Chem. 274 (1999) 34233–34237.
[37] M.E. Mosher, L.K. White, J. Hermolin, R.H. Fillingame, H^+-ATPase of *Escherichia coli*. An *unc*E mutation impairing coupling between F_1 and Fo but not Fo-mediated H^+ translocation, J. Biol. Chem. 260 (1985) 4807–4814.